Archives of Hydro-Engineering and Environmental Mechanics
Vol. 42 (1995), No. 1–2, pp. 3–27

Nonlinear Effects of Waves and Currents on Moveable Bed Roughness and Friction

Leszek M. Kaczmarek

Institute of Hydro-Engineering Polish Academy of Sciences, ul. Kościerska 7,
80–953 Gdańsk, Poland

(Received March 01, 1995; revised June 30, 1995)

Abstract

A new theoretical approach based on the grain-grain interaction ideas is proposed for the evaluation of moveable bed roughness under regular and irregular waves, sinusoidal/asymmetric waves with/versus currents. This method uses Coulomb friction between particles (plastic stresses) with viscous-type stresses for particle collision stresses to represent seabed drag effects in a similar way to the flow of cohesionless material. By using an iterative procedure to balance the overall drag the bed roughness is related to the applied hydrodynamic stress and hence the external wave field. The theoretical bed level is defined by the matching point of the logarithmic distribution with the sub–bed flow profile. For the moment when maximum shear stress occurs the continuity of shear stress and velocity at the theoretical bed level is required.

The ability of the proposed iterative procedure to evaluate the roughness parameter has been checked for sandy bed with various grain diameters and various regular and irregular wave conditions. The proposed approach explains the reduction of spectral wave friction factors. The various aspects of the nonlinearity in respect to moveable bed roughness including the asymmetry of waves and the interactions between asymmetric waves and currents are discussed.

1. Introduction

A wide variety of coastal problems rely on accurate prediction of sediment transport in response to the action of waves and currents. However, the prediction of the effect of waves on sediment transport is still generally restricted to monochromatic, unidirectional, non-breaking waves. In real sea conditions, where irregular waves are observed, the nonlinear process of sediment transport may respond in a rather different way to the idealized regular wave case. Other aspects such as wave-breaking and wave asymmetry are also important in terms of sediment transport, particularly in shallow water as in the coastal environment.

In shallow coastal waters the flow and the sediment transport are largely controlled by friction. Consequently, the computations of these quantities are found

to depend strongly on the bed roughness, parameterized by the seabed drag coefficient, the bottom equivalent roughness, or the bed roughness length z_0.

For a turbulent flow over the seabed, the velocity profile in the near-bed region can be represented by the familiar von Karman-Prandtl equation:

$$u(z) = \frac{u_f}{\kappa} \ln \frac{z}{z_0} \tag{1}$$

where $u(z)$ is the fluid velocity at height z above the bed, κ is von Karman's constant (≈ 0.4) and u_f the friction velocity, while the bed roughness length z_0 is related to the apparent (Nikuradse equivalent) roughness k_a by the relation:

$$z_0 = \frac{k_a}{30}. \tag{2}$$

The specification of the roughness is, however, a major source of uncertainty. Generally speaking velocity profile measurements made close to the sea bed are found to fit Equation (1) by plotting as a straigth line on u versus ln z axis. A least squares technique can then be used to obtain the best fit of Equation (1) to the measurements, the gradient of the fitted profile gives u_f and the intercept of the profile with z-axis yields the roughness length z_0 the height above the bed where the velocity extrapolates to zero.

The uncertainty of applying laboratory derived values or relationships for k_a to seabed sediments has meant that in practice it is probably safest to estimate k_a from velocity profile measurements made in the sea if they are available. The complications in determining u_f and k_a once sediment is in motion have been summarised previously by Soulsby et al. (1983):

a) the ripple geometry may change with time causing variations in z_0,
b) the saltations of grains along the bed enhance the momentum transfer from, the flow to the bed, causing an increase in z_0.
c) the suspended sediment in the water column produces a vertical density gradient and hence a departure from Equation (1).

Consequently the present study looks for a simple way to predict the moveable bed roughness under regular and irregular waves, symmetrical waves with/versus or without currents, from a small number of available velocity parameters.

To parameterize the roughness parameter k_a in terms of the wave spectrum and a few other parameters, it is necessary to start from the surface elevation spectrum which must be transformed into orbital velocities at the bed and then to bed shear stress which is used in a sediment transport formula. This route from surface elevation to sediment transport is shown in Fig. 1 (Ockenden and Soulsby, 1994). The problem is highly nonlinear and the importance of the nonlinearity is therefore central to this study.

At three points in the process it is necessary to make nonlinear transformations (Fig. 1). Additionally to three nonlinear transformations there is another one due to the nonlinear character of the near bed interactions between water motion and the seabed itself. These interdependencies, described by items (a) – (c), can be expressed by the following relationship:

$$z_0 = \frac{k_a}{30} = f(u_f, s, d), \tag{3}$$

where: s – specific grain density (2.66), d – grain diameter.

The determination of the function f in Equation (3) requires the formulation of the model of a boundary layer and sediment movement accounting for normal and shear stress generation in the soil by surface waves.

To this end, a new theoretical approach based on the grain-grain interactions idea is proposed. This approach follows the earlier method described by Kaczmarek and O'Connor (1993a, b) for sheet-flow and rippled-bed conditions under regular waves respectively and the Kaczmarek et al. method (1994) for spectral waves.

This method uses Coulomb friction between particles (plastic stresses) with viscous-type stresses for particle collision stresses to represent seabed drag effects in a similar way to the flow of cohesionless material. By using an iterative procedure to balance the overall drag, it is possible to relate the bed roughness to the applied hydrodynamics stress and hence the external wave field.

The method for spectral waves is based on the methodology which assumes that the spectral wave condition can be represented by a monochromatic wave and includes the suggestion of Madsen et al. (1990), that the longer waves in a spectral simulation shave off the sharp ripple crests, thereby causing the observed reduction in dissipation and friction factors.

The various aspects of the nonlinearity in respect of moveable bed, roughness and friction are discussed, including the asymmetry of waves (described by Stokes' second and third theory) and the interactions between asymmetric waves and/versus currents.

2. Moveable Bed Boundary Layer Model

2.1. Formulation of the Problem

A typical velocity vertical distribution of a rough bed is supposed to be characterized, cf. Kaczmarek and O'Connor (1993a, b), by a sub-bottom flow and a main or outer flow, as shown in Fig. 2.

The velocity distribution is supposed to be continuous. Its intersection with the nominal bottom is the apparent slip velocity u_b. The downward extension of the velocity distribution in the outer zone of the main flow yields a fictitious slip velocity u_0 at the nominal bed, which is necessarily greater than u_b because of the

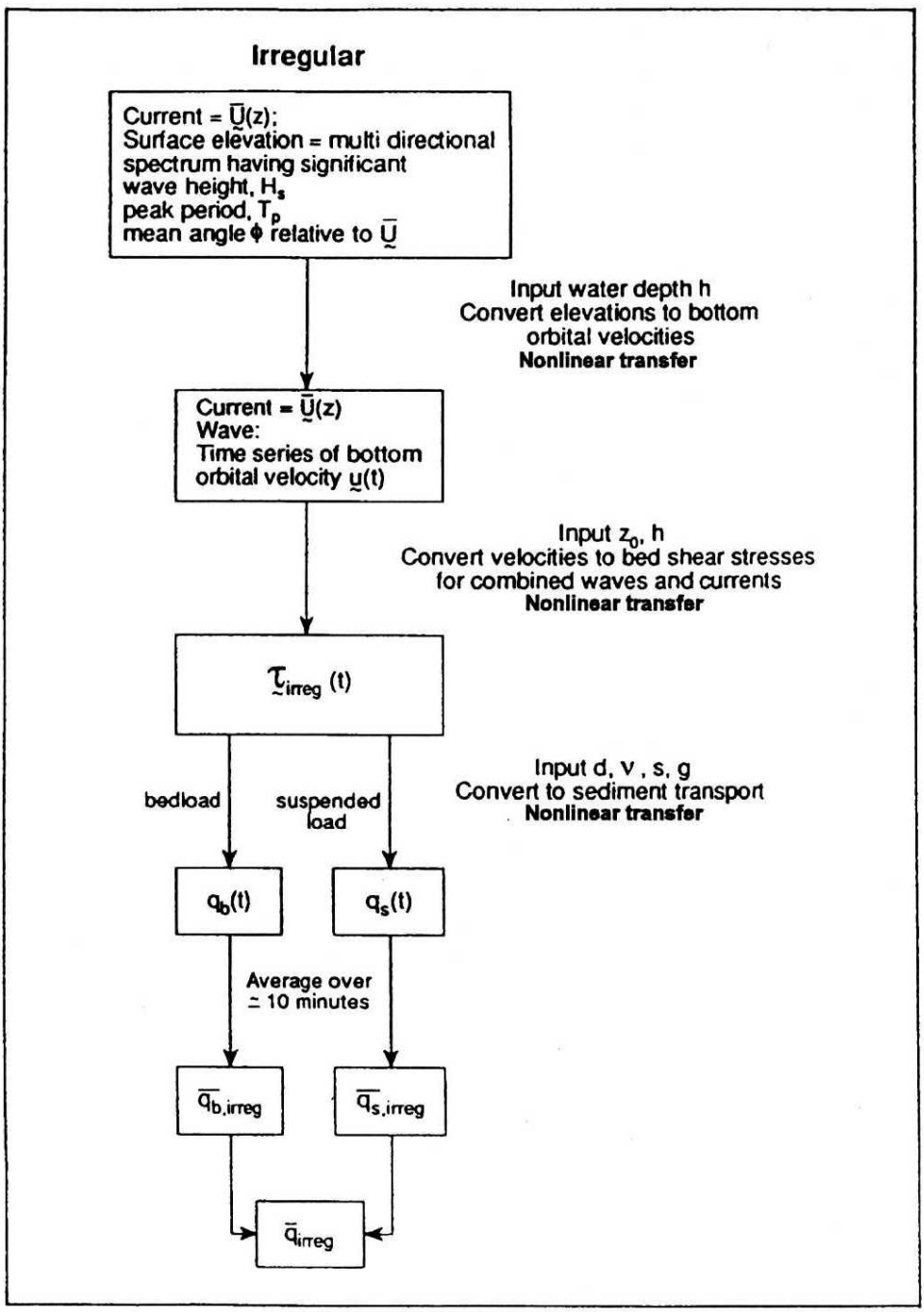

Fig. 1. The nonlinear route from surface elevation to sediment transport, after Ockenden and Soulsby (1994)

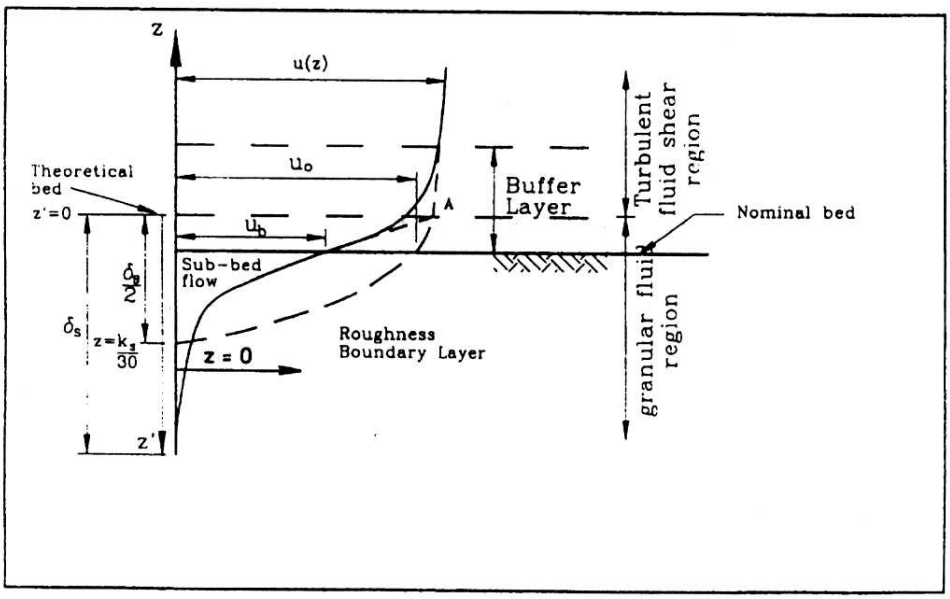

Fig. 2. Definition sketch of turbulent flow over a moveable bed

supposedly asymptotic transition in the buffer layer between the sub-bed flow and the fully turbulent flow in the turbulent-fluid shear region.

The velocity distribution in the roughness layer depends on the type of geometric roughness pattern and the bed permeability. There must be some transition between both parts of the velocity distribution in the buffer zone. However, for present purposes it is assumed that the velocity distribution in the turbulent-fluid shear region can be determined by parameters depending on the geometric roughness properties of the bed and outer flow parameters, such as the free-stream wave velocity. It is proposed to extend the sub-bed granular-fluid flow region to the matching point with the velocity distribution in the turbulent-fluid shear region. Thus shear stress velocities in the two layers are set equal at the theoretical bed level, as is shown in Fig. 2, point A.

The first problem, therefore, is to determine the distribution of the velocity profile in the upper turbulent layer, which means determining the effective roughness height of the bed k_a as well as in the lower grain-fluid flow layer. The intersection of these two profiles will determine point A in Fig. 2.

2.2. Mathematical Description of the Flow in the Granular-Fluid Region

Particle interactions in the shear-grain-fluid flow are assumed to produce two distinct types of behaviour. The Coulomb friction between particles give rise to rate-independent stresses (of the plastic type) and the particle collisions give rise to stresses that are rate-dependent (of the viscous type). We assume the co-existence

of both types of behaviour and the stress tensor is divided into two parts:

$$\sigma_{ij} = \sigma_{ij}^0 + \sigma_{ij}^* \tag{4}$$

where σ_{ij}^0 is the plastic stress and σ_{ij}^* is the viscous stress.

For two-dimensional deformation in the rectangular Cartesian co-ordinates x' and z', the Coulomb yield criterion is satisfied by employing the following stress relations:

$$\sigma_{x'x'}^0 = -\sigma^1(1 + \sin\varphi\cos 2\psi), \tag{5}$$

$$\sigma_{z'z'}^0 = -\sigma^1(1 - \sin\varphi\cos 2\psi), \tag{6}$$

$$\sigma_{x'z'}^0 = -\sigma^1 \sin\varphi \sin 2\psi. \tag{7}$$

Where φ is the quasi-static angle of internal friction, while ψ denoting the angle between the major principal stress and the x'-axis is equal to:

$$\psi = \frac{\pi}{4} - \frac{\varphi}{2}.$$

For the average normal stress:

$$\sigma^1 = -\left(\frac{\sigma_{x'x'}^0 + \sigma_{z'z'}^0}{2}\right) \tag{8}$$

we employ the following approximate expression (Sayed and Savage 1983).

$$\sigma^1 = \alpha^0\left(\frac{c - c_0}{c_m - c}\right) \tag{9}$$

where α^0 is a constant and c_0 and c_m are the concentrations of solids corresponding to fluidity and closest packing, respectively.

The viscous part of the stress tensor according to Sayed and Savage (1983) is assumed to have the following form:

$$\sigma_{x'x'}^* = \sigma_{z'z'}^* = -(\mu_0 + \mu_2)\left(\frac{\partial u}{\partial z'}\right)^2, \tag{10}$$

$$\sigma_{x'z'}^* = \sigma_{z'x'}^* = \mu_1\left|\frac{\partial u}{\partial z'}\right|\frac{\partial u}{\partial z'} \tag{11}$$

in which the viscous stress coefficients μ_0, μ_1 and μ_2 are functions of the concentration of solids c:

$$\frac{\mu_1}{\rho_s d^2} = \frac{0.03}{(c_m - c)^{1.5}}, \tag{12}$$

$$\frac{\mu_0 + \mu_2}{\rho_s d^2} = \frac{0.02}{(c_m - c)^{1.75}} \tag{13}$$

where ρ_s and d are the mass density and diameter of the solid particles.

Considering steady fully developed two-dimensional shear-grain-flow, the balance of linear momentum according to Kaczmarek and O'Connor (1993a, b) yields:

$$\alpha^0 \left[\frac{c - c_0}{c_m - c}\right] \sin\varphi \sin 2\psi + \mu_1 \left[\frac{\partial u}{\partial z'}\right]^2 = \rho u_f^2, \tag{14}$$

$$\alpha^0 \left[\frac{c - c_0}{c_m - c}\right] (1 - \sin\varphi \sin 2\psi) + (\mu_0 + \mu_2) \left[\frac{\partial u}{\partial z'}\right]^2 =$$

$$= \left[\frac{\mu_0 + \mu_2}{\mu_1}\right]_{c=c_0} \rho u_f^2 + (\rho_s - \rho) g \int_0^{z'} c dz' \tag{15}$$

where ρ is the density of the fluid.

Eliminating $(\partial u/\partial z')^2$ from Equations (14) and (15) gives:

$$\alpha^0 \left(\frac{c - c_0}{c_m - c}\right) \left[1 - \sin\varphi \cos 2\psi - \left(\frac{\mu_0 + \mu_2}{\mu_1}\right) \sin\varphi \sin 2\psi\right] =$$

$$= \rho u_f^2 \left\{\left[\frac{\mu_0 + \mu_2}{\mu_0}\right]_{c=c_0} - \left[\frac{\mu_0 + \mu_2}{\mu_1}\right]\right\} + (\rho_s - \rho) g \int_0^{z'} c dz'. \tag{16}$$

The system of Equations (14) and (15) enables the calculation of the profiles of the sub-bed sediment concentration c and velocity u in relation to known maximum shear stress $(\rho u_{f\,\max}^2)$ at the theoretical bed level $(z' = 0)$.

In Kaczmarek and O'Connor (1993a, b) Equation (16) was solved for c as a function of depth (z') by using an iteration method in conjunction with numerical integration. Integration started at the theoretical bed level $(z' = 0)$ with $c = c_0$. Proceeding downwards at each step the iteration method was used to evaluate c. Integration was stopped when c was equal to c_{ms}. For the calculations the following numerical values were recommended for the various parameters:

$$\frac{\alpha^0}{\rho_s g d} = 1, \quad c_0 = 0.32, \quad c_m = 0.53, \quad c_{ms} = 0.50. \tag{17a}$$

Typical stress distribution in the sub-bed flow layer for the ripple-bed conditions (Kaczmarek and O'Connor 1993b) is shown in Fig. 3a, while – for the sheet flow conditions (Kaczmarek and O'Connor 1993a) – in Fig. 4a. The typical velocity and concentration of solids profiles for rippled-bed and sheet flow are presented in Fig. 3b and 4b, respectively. The calculations were carried out for a sand bed, characterised by the parameters:

$$s = \frac{\rho_s}{\rho} = 2.66, \quad \varphi = 24.4°. \tag{17b}$$

Note that the concentration of solids increases downwards the bed and the introduction of the fictitious flow for rippled-bed condition (see discussion in Kaczmarek and O'Connor 1993b) provides this increase up to the value of $c_{ms} = 0.50$, where the particles lock together and where the momentum is transferred only by the Coulomb friction between them. Finally, it allows the inclusion of the seepage flow effect on the roughness parameter k_a.

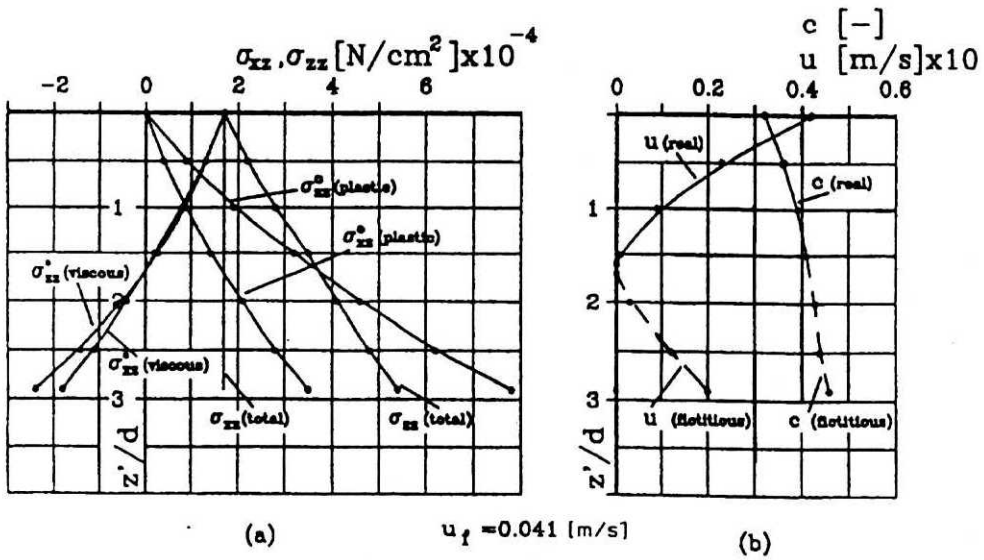

Fig. 3. Exemplary computed stresses (a), velocity and concentration (b) in the sub-bed layer for the rippled bed conditions

2.3. Mathematical Description of the Flow in the Turbulent Upper Region

The quantity $u_{f\,\max}$ is postulated to be determined from the solution of the integral equation derived by Fredsoe (1984):

$$\frac{\tau(\delta)}{\rho} - \frac{\tau_0}{\rho} = -\int_{\frac{k_a}{30}}^{\delta+\frac{k_a}{30}} \frac{\partial}{\partial t}(U-u)dz \tag{18}$$

where $U(t)$ is the free stream velocity, τ_0 is the bed shear stress and $\tau(\delta)$ is the shear stress at the top of the boundary layer, resulting from the mean current (if present).

Fredsoe (1984) assumed that the velocity profile in the boundary layer is described by the logarithmic function:

$$\frac{u}{u_f} = \frac{1}{\kappa} \ln \frac{30z}{k_a}. \tag{19}$$

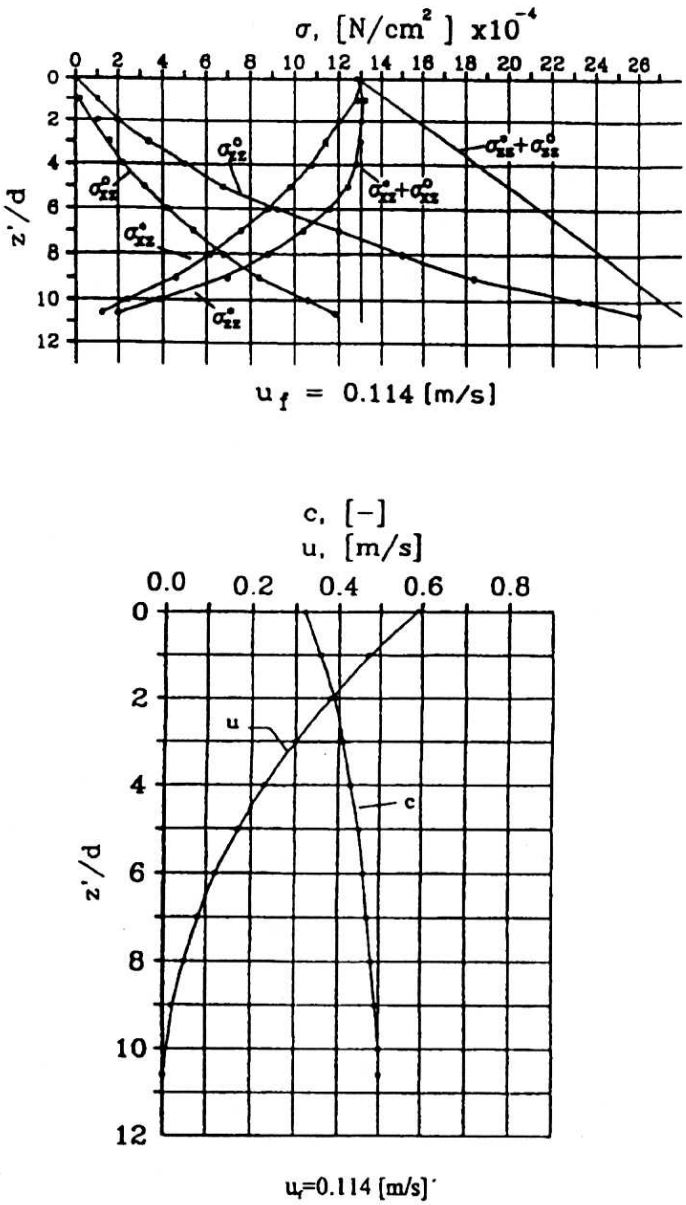

Fig. 4. Exemplary computed viscous and plastic stresses (top), velocity and concentration in the sub-bed layer (bottom) for the sheet flow conditions

The boundary condition at the upper limit of the boundary layer reads $u = U$ at $z = \delta + \frac{k_a}{30}$. On the strength of Equation (19) one has:

$$\delta = \frac{k_a}{30}(e^{z_1} - 1) \tag{20}$$

in which

$$z_1 = \frac{U_\kappa}{u_f \mp u_{f0}} \tag{21}$$

where $u_{f0} = [\pm\tau(\delta)]^{0.5}$.

Fredsoe (1984), using the derivative of Equation (21) after re-arranging the integral on the right side of Equation (18), obtained the differential equations

$$\frac{dz_1}{d(\omega t)} = \frac{30\kappa^2 U(\omega t)}{k_s \omega e^{z_1}(z_1 - 1) + 1} - \frac{z_1(e^{z_1} - z_1 - 1)}{e^{z_1}(z_1 - 1) + 1} \cdot \frac{1}{U} \cdot \frac{dU}{d(\omega t)}, \tag{22}$$

$$\frac{dz_1}{d(\omega t)} = \frac{30 z_1^2 \left[\left|\frac{\kappa U}{z_1} \mp u_{f0}\right| \left(\frac{\kappa U}{z} \pm u_{f0}\right) \pm u_{f0}^2\right]}{\omega k_s U[e^{z_1}(z_1 - 1) + 1]} - \frac{z_1(e^{z_1} - z_1 - 1)}{e^{z_1}(z_1 - 1) + 1} \cdot \frac{1}{U} \cdot \frac{dU}{d(\omega t)} \tag{23}$$

for pure wave motion and wave with/against current, respectively.

The solution of Equations (22) and (23) was achieved by the Runge-Kutta second-order method. As a result, the function $z_1(t)$ was obtained and the time distributions of the friction velocity $u_f(t)$ and boundary layer thickness $\delta(t)$ calculated thereafter on the basis of Equations (20) and (21).

It should be emphasized that the free stream velocity $U(t)$ can be described as linear or nonlinear, thus Fredsoe's model can be adapted to nonlinear (asymmetric) wave/wave-current motion, cf. Kaczmarek and Ostrowski (1992).

The solution of Equations (22) and (23) enables the value of $u_{f\max}$ to be determined, if k_a is specified. To evaluate the roughness parameter k_a an iterative procedure is proposed for finding the matching point A.

The entire velocity distribution is supposed to be continuous and the velocity distribution in the outer zone of the main flow to be logarithmic.

Thus, the theoretical bed level is defined by the matching point A of the logarithmic distribution with the sub-bed flow profile (Fig. 2). It is assumed that the matching point A is when the maximum (in wave-current period) shear stress $pu_{f\max}^2$ occurs. Hence, for the moment when maximum shear stress occurs the continuity of shear stress and velocity at the theoretical bed level is required. It is assumed that both the logarithmic and sub-bed profiles depend on the values of k_a. The calculations are stopped when the velocity at the top of the sub-bed layer reaches the value determined by the logarithmic distribution, at the $\delta_s/2$ level. The thickness $\delta_s/2$ of the downward extension of the logarithmic distribution from matching point A was chosen rather arbitrarily. However, this value yielded flow

predictions which were in reasonable agreement, cf. Kaczmarek and O'Connor (1993a), with the experimental results of Horikawa et al. (1982). The value of δ_s is the thickness of concentration in the sub-bed flow layer.

The existence of a logarithmic layer corresponding to Equation (19) is not always equally obvious in the experimental data, cf. Nielsen (1992), and in some cases the fitting of a logarithmic layer is somewhat arbitrary. However, in order to formulate simple models of natural flows it is generally necessary to apply a simplified description of the bed geometry, and in extreme cases one often tries to summarize the bed geometry in terms of a single length, i.e. equivalent Nikuradse roughness.

Generally, the existing models for oscillatory boundary layers fall into two broad physical categories, namely horizontally uniform models where $u = u(z, t)$ and models which take into account the horizontal variability of $u(x, z, t)$ (see Fig. 5) between crests and troughs of the bed roughness elements. The latter group is by far the smallest although realistic modelling of the flow over the commonly observed sand ripples obviously calls for models which can describe localized vortex formation.

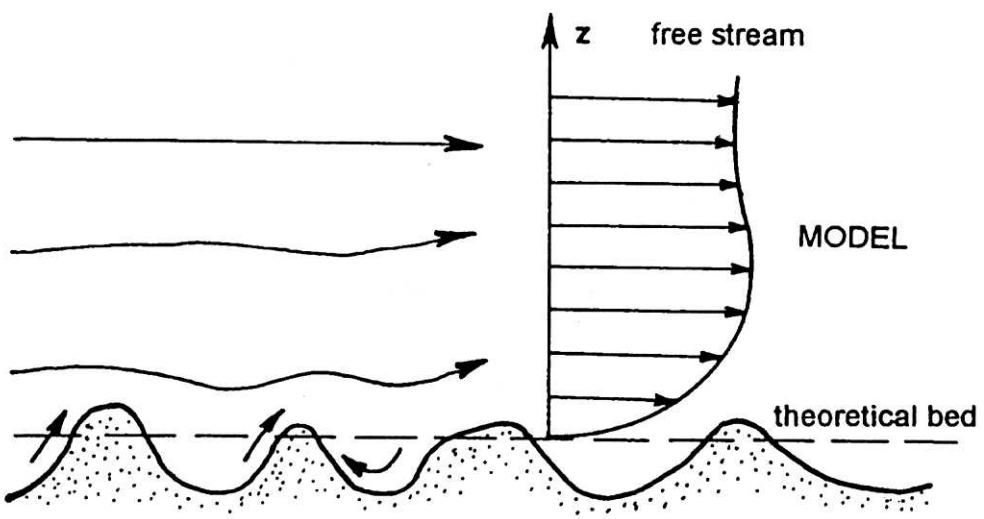

Fig. 5. Definition sketch for horizontally averaged model over rippled bed

Horizontally uniform models are much simpler. They can, however, only be literally valid at elevations which are well clear of the top of the roughness elements, i.e. for $z \gg k_a$. Hence, unless $\delta \gg k_a$ they are at most relevant as descriptions of the horizontal average of the flow.

The viability of the assumption of a logarythmic velocity distribution at all phases of the flow depends on the relative roughness k_a/a_{1m}. Rippled sand beds generally gave $k_a/a_{1m} > 0.2$. This value is only meant as an indication. The choice

of an upper limit of k_a/a_{1m} for the application of horizontally averaged models does of course, in the end, depend on the amount of details one needs to consider.

3. Results of Computations

3.1. Regular Waves

The ability of the proposed iteration procedure to evaluate the roughness parameter k_a has been checked for a sandy bed ($s = \rho_s/\rho = 2.66$; $\varphi = 24.4°$) with different grain diameter d and various wave conditions. The results of the computations are plotted in Fig. 6, together with the results for irregular waves which are discussed in section 3.2.

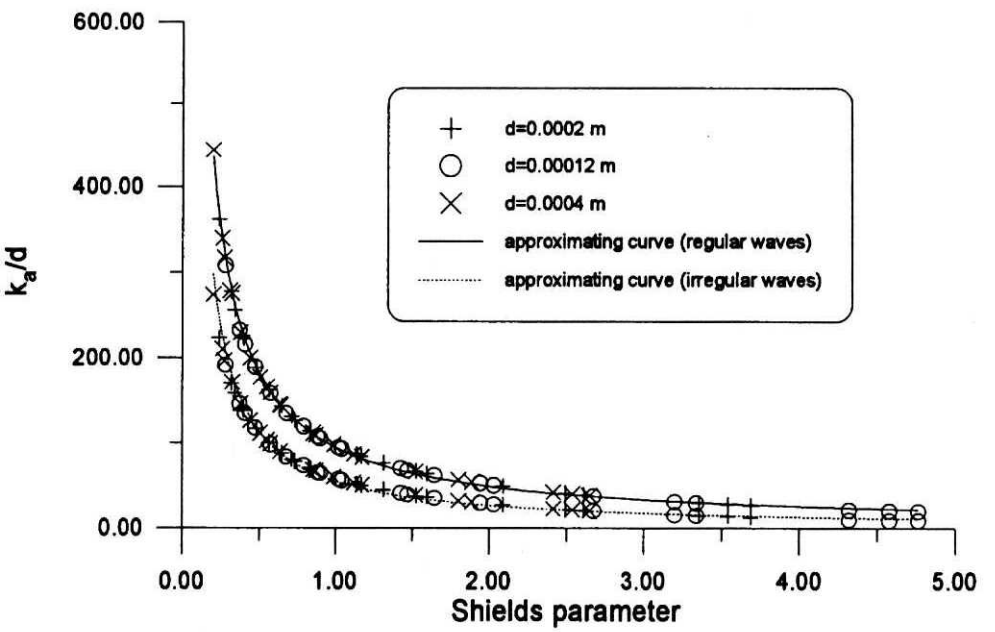

Fig. 6. Computed roughness parameter k_a for regular and irregular waves

The present results show quite the opposite trend of the behaviour of the roughness parameter to those suggested by many authors, where the roughness parameter increases drastically with increasing transport intensity. Here, it is seen that the roughness parameter decreases with increasing dimensionless maximum bed shear stress $\theta_{\max}$ (Shields parameter) defined as:

$$\theta_{\max} = \frac{u_{f\max}^2}{(s-1)gd}. \tag{24}$$

Providing that $\theta_{\max}(u_{f\max})$ is obtained using the proposed model, i.e. Equations (21), (22) and (23), it is worth giving an approximating formula for the

purpose of engineering applications:

$$\log\left[\frac{k_a}{d}\right] = -0.95\log[\theta_{\max}] + 4.55. \tag{25}$$

The ability of the present theoretical approach to predict the roughness height for rippled bed conditions is demonstrated here using the laboratory data reported by Madsen et al. (1990). The experimental values of the wave friction factors f_w, obtained for the monochromatic waves are presented in Fig. 7 versus the representative value of a fluid-sediment interaction parameter:

$$S_r = \frac{\psi'_{mr}}{\psi_c} \tag{26}$$

in which

$$\psi'_{mr} = \frac{u'^2_{f\max}}{(s-1)gd} \tag{27}$$

is the Shields parameter obtained from the maximum bottom skin shear stress based on grain-size bed roughness, i.e. for $k_a = d$, and ψ_c is the critical value of Shields parameter for initiation of sediment motion. Thus the parameter S_r represents the extent to which threshold conditions are exceeded.

The calculations of the friction factors were carried out in two steps. First, the values of the bed roughness k_a were obtained using the proposed iterative scheme. Then, the friction factors were calculated on the basis of adjusted semi-empirical formula of Jonsson and Carlsen (1976).

$$\frac{1}{4\sqrt{f_w}} + \log\frac{1}{4\sqrt{f_w}} = -0.08 + \log\frac{a_{1m}}{k_a} \tag{28}$$

to include the contribution of the vortices formation in the lee of the roughness crest to the shear stress.

Here Equation (28) was proposed for the calculations of both the friction factors and the skin shear stresses $\rho u'^2_{f\max}$ defined by Equation (27) and the following formula:

$$f_w = \frac{2u^2_{f\max}}{U^2_{1m}} = 2\left(\frac{u_{f\max}}{U_{1m}}\right)^2. \tag{29}$$

The calculations were performed for two different sediments (0.2 mm and 0.12 mm diameter quartz sands). The theoretical results are shown in Fig. 7. The results for irregular waves, although discussed later – in section 3.2, are also included in Fig. 7 for the sake of full comparison. The agreement between theoretical and experimental results appears to be quite satisfactory.

The ability of the present theoretical approach to predict the roughness height in the plane-permeable bed conditions is demonstrated here using the

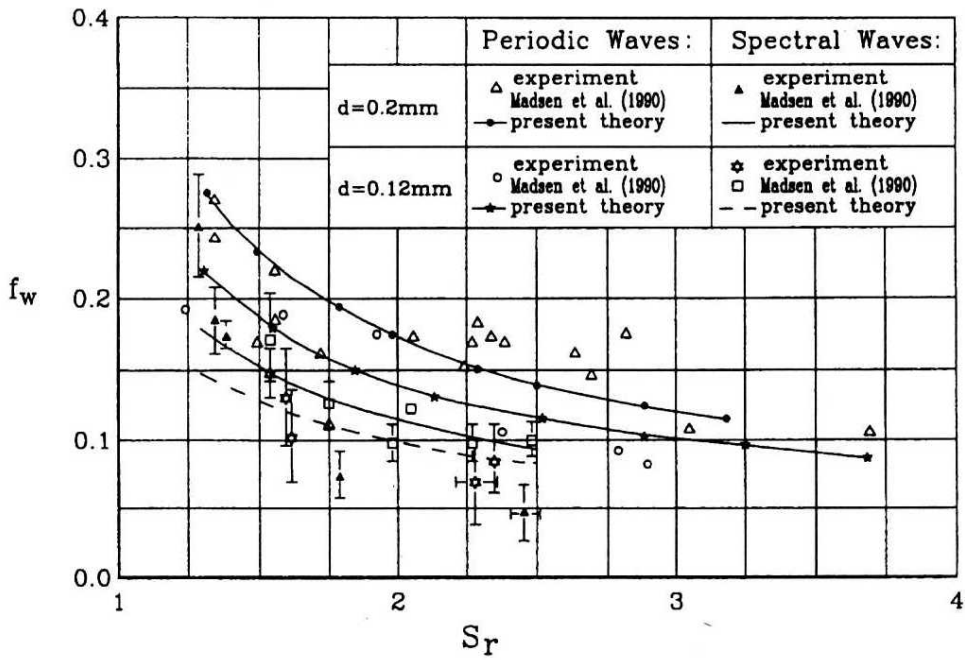

Fig. 7. Moveable bed friction factors for regular and irregular waves

field measurements of large wave boundary layers made by Myrhaug et al. (1992) and VWS laboratory tests reported by Oebius (1992). The experimental data of Myrhaug et al. (1992) were collected in two different measurements programs, the Pipeline Field Measurement Program (PFMP) and the Pipeline Design Project (PIPESTAB).

During the PFMP measurements the sea floor was characterized as generally flat and rough, consisting of rock and gravel bed sediments. For the PIPESTAB measurements the sea floor was generally flat and uniform, consisting mainly of fine sand. However, during storms, ripples were formed. A characteristic grain size diameter (d_{50}) for the bottom sediment was 0.20 mm.

According to the present theoretical approach one may expect small values of a_{1m}/k_a for the case of a plane-permeable bottom. However, because the bed remains flat it is expected that the geometrical scale of the roughness elements (the sediment diameter) is at least an order of magnitude smaller than the thickness of the turbulent boundary layer. Thus, the separation flow effects over the roughness elements are negligible compared with the turbulent eddies connected with the bed shear stresses. It was suggested by Kaczmarek and O'Connor (1993b) that for such bed flow conditions the standard turbulent models can accurately predict the friction factors. Indeed, the theoretical values of friction factor obtained by use of Fredsoe's (1984) model, plotted in Fig. 8, show good agreement with the analysis results from the measurements made by Myrhaug et al. (1992). Consistency was

also found by Myrhaug et al. (1992) between the analysis results from the field data and those from large and small scale laboratory tests with sinusoidal oscillations (see Fig. 8). The theoretical values obtained by Myrhaug et al. (1992) on the basis of their semi-empirical relationships are also included in Fig. 8.

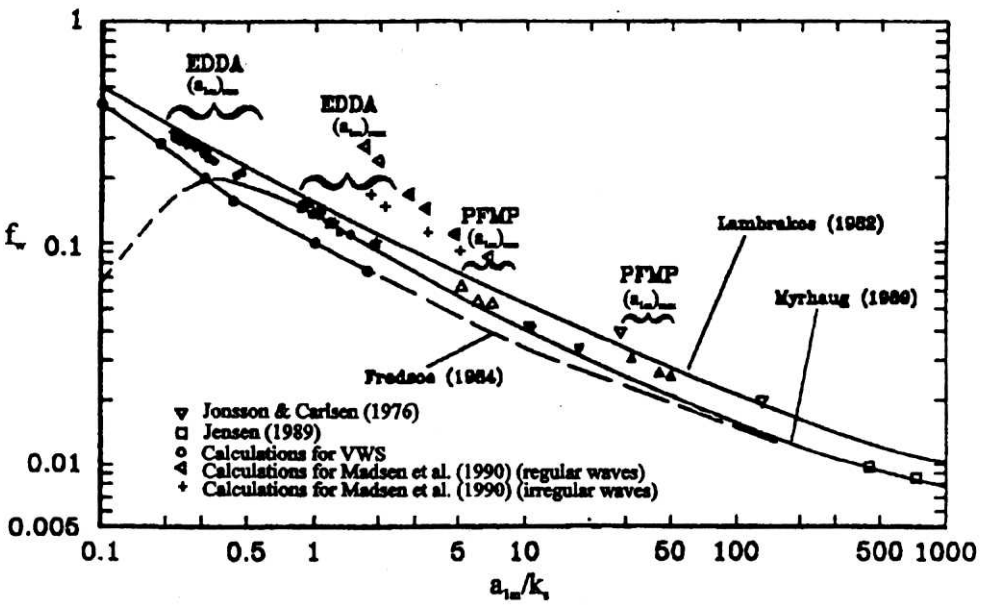

Fig. 8. Wave friction coefficient versus amplitude-to-roughness ratio

For comparison, the theoretical results of the friction factors obtained using the proposed iterative scheme for laboratory data of Madsen et al. (1990) and for VWS laboratory tests of Oebius (1992) are also shown in Fig. 8.

The VWS report deals with development, design, construction and the testing of an *in situ* shear stress meter, which is able to measure horizontal as well as vertical shear force components. Coarse bed materials were used in the VWS laboratory tests which were carried out under different sediment and velocity conditions, but below the threshold for incipient motion of the sediment. The measurements were carried out with a rigid shear plate made from aluminium and covered with sediment of the same type as used for the surrounding sediment bed. The different configuration of shear plates and casings (rigid and porous structures) were constructed and investigated.

The results of the calculations of the shear stresses, on the basis of the iterative procedure are shown in Fig. 9 in comparison with the measurements made by Oebius (1992). Again, agreement between theoretical and experimental results appears to be quite satisfactory, although considerable scatter of the experimental points is observed.

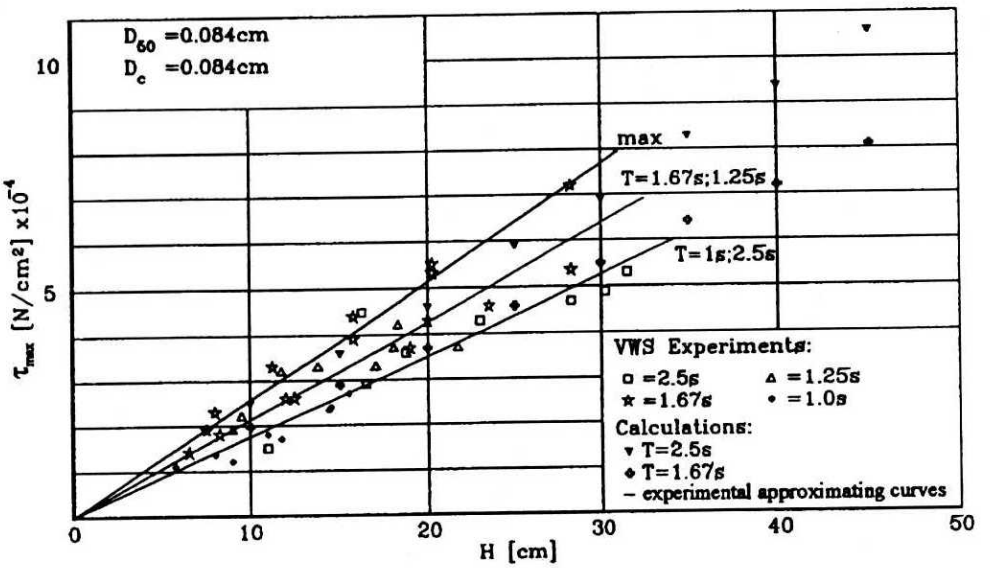

Fig. 9. Horizontal shear stress for waves over a permeable-flat bed

Basing on the present analysis it is not possible to arrive at a definite conclusion as to how an irregular sea state should be represented. However, it should be mentioned that for large wave activity during measurements in the North Sea, ripples were formed. It indicates that for such conditions the wave friction coefficient f_w should be described better by the Jonsson and Carlsen (1976) (or Kamphuis 1975) formulae rather than by the Fredsoe (1984) turbulence model. It was not confirmed, however, by the experimental data (see Fig. 8). In an attempt to explain the behaviour of the friction coefficient the reduction of spectral wave friction should be taken into consideration. The reduction of spectral wave friction factors considerably below the values of their monochromatic counterparts was experimentally detected by Madsen et al. (1990) (see Fig. 7).

3.2. Irregular (Spectral) Waves

The effect of random waves on bed roughness needs to be studied, since it is known that the bed friction changes between mono-frequency and random conditions. The Madsen et al. (1990) hypothesis is that the larger waves in a spectral simulation shave off the sharp ripple crests thereby causing the observed reduction in dissipation and friction factor for spectral waves. In an attempt to explain this reduction of spectral wave friction factors a new theoretical approach for predictive evaluation of moveable bed roughness for spectral waves is proposed (Kaczmarek et al. 1994). The new approach is based on the method which assumes that the spectral wave condition can be represented by a monochromatic wave and is combined with the theoretical grain-grain interaction ideas.

By analogy to a monochromatic wave, one may expect the following relationship between the irregular input specified by the root-mean-square free stream velocity amplitude U_{rms} (equal to $\sqrt{2}$ times the standard deviation, σ_U, of the free stream velocity series) and the irregular output specified by the root-mean-square bed shear stress amplitude τ_{rms} (equal to $\sqrt{2}$ times the standard deviation, σ_τ, of the bed shear stress series):

$$\tau_{rms1,2} = F_{1,2}[U_{rms}, T_r, k_a = f(\tau_{\max 1}, s, d)] \tag{30}$$

where subscripts 1 and 2 refer to the plane and rippled bed, respectively.

To calculate the function F, Fredsoe's (1984) boundary layer model is recommended in the case of flat bed ($F_1 \rightarrow \tau_{\max 1}$) while the empirical formula of Kamphuis (1975) or semi-empirical equation of Jonsson and Carlsen (1976) are postulated for rippled bed conditions ($F_2 \rightarrow \tau_{\max 2}$) in order to include the effects of the vortices formed in the lee of the roughness element crest due to turbulent mixing.

Under monochromatic waves the maximum shear stress is the maximum value of shear stress during a wave period, while for spectral waves it becomes the maximum value of the random shear stress time series. To calculate this value it is proposed to use the following simple relation (Kaczmarek et al. 1994):

$$\tau_{\max} \frac{3\tau_{rms}}{\sqrt{2}} = 3\sigma_\tau. \tag{31}$$

The choice is fairly arbitrary, however, and it will be shown later that it yields the best agreement of the calculations using Madsen et al. (1990) data.

Thus, the procedure is proposed for determination of bed roughness under irregular waves. The procedure incorporates the iterative method described in section 2.3. The concise computational scheme is given in Fig. 10.

The value T_r is the period of the monochromatic wave which represents the random wave field. However, the question of which equivalent (representative) wave period to choose to represent the spectral wave condition still seems to exist.

The problem is very sophisticated and requires a separate analysis. Here, it is worth referring the reader to the studies of Kaczmarek et al. (1994) and Kaczmarek and Ostrowski (1994), in which a combination of Fredsoe's (1984) and Brevik's (1981) solutions and a $k - \epsilon$ boundary layer model are being used, respectively, to study the best representative wave.

The first method, i.e. Kaczmarek and Ostrowski (1994), uses a combination of Fredsoe's (1981) and Brevik's (1984) solutions to describe each harmonic component of the wave motion. A coupling exists between the component of the wave motion. There is a coupling between the components incorporated in the eddy viscosity modelling. A simple time-invariant eddy viscosity formulation is assumed valid. However, in contrast to Madsen et al. (1988), a two-layer eddy viscosity

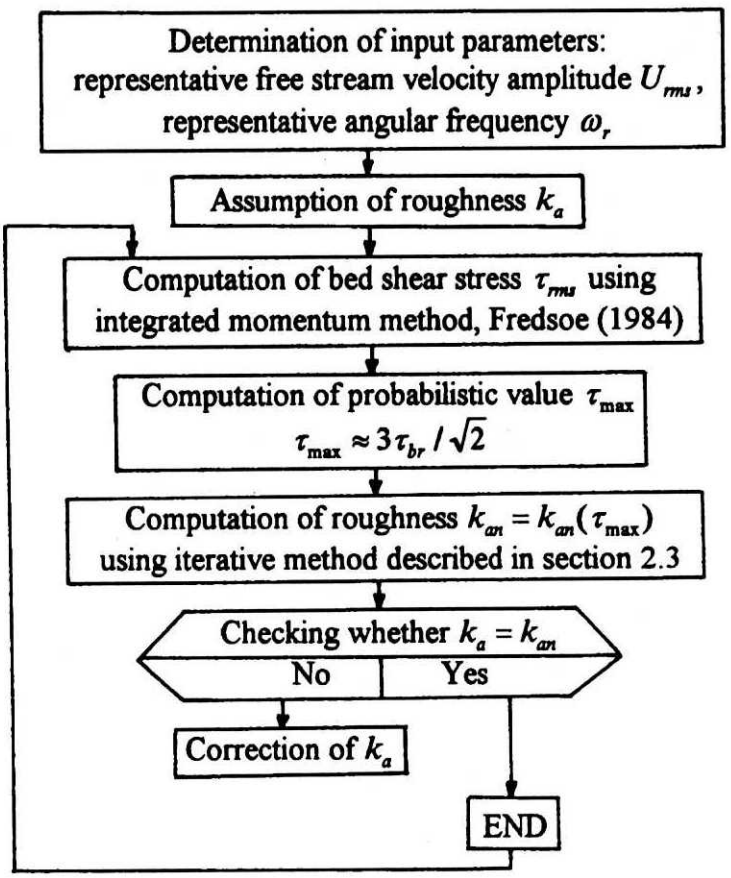

Fig. 10. Computational scheme

model is proposed. The problem is closed by an iterative scheme for finding the wave period representing the random wave field.

The second approach, i.e. Kaczmarek et al. (1994), follows the earlier method of O'Connor et al. (1992) but using a $k-\epsilon$ boundary layer model to study the best representative wave.

The ability of the present approach to evaluate moveable bed roughness, k_a under spectral waves was checked for a sandy bed: $s = \rho_s/\rho = 2.66$, $\varphi = 24.4°$ with different grain size and various wave conditions. The results of the computations are plotted in Fig. 6, together with the results for regular waves.

The following approximating formula:

$$\log\left[\frac{k_a}{d}\right] = -1.05\log[\theta_{rms}] + 4.00 \tag{32}$$

differs slightly from the formula for monochromatic waves described by Equation (25) (see Fig. 6) because the largest waves in a spectral simulation (described by

Equation (31)) shave off the sharp ripple crests thereby causing the reduction in the roughness parameter.

In an attempt to explain the reduction of spectral wave friction factors the present theoretical approach was run with Madsen et al. (1990) laboratory data. The theoretical values of the wave friction factors f_w are presented in Fig. 7, plotted against the representative value of a fluid-sediment parameter, in which the Shields skin parameter defined for spectral waves as:

$$\theta' = \frac{\tau'_{rms}}{\rho(s-1)gd} \tag{33}$$

is obtained from the bottom skin shear stress based on grain-size bed roughness, i.e. for $k_a = d$.

The calculations of the friction factors for irregular waves were carried out in a similar manner as those for regular waves involving two steps. First, the values of the bed roughness k_a were obtained using the proposed computational method (Fig. 10) with Fredsoe's (1984) model used to determine the bed shear stress, τ_{mrs}. Then the friction factors were calculated on the basis of the adjusted semi-empirical formula of Jonsson and Carlsen (1976) in order to include the contribution of vortex formation in the lee of the roughness crests to the shear stress. Here, the Jonsson and Carlsen (1976) formula was proposed for the calculation of both the friction factors and the dimensionless skin shear stress.

The agreement between theoretical and experimental results again appears to be satisfactory. Thus the reduction of spectral wave friction factors considerably below the values of their monochromatic counterparts, can explain the fact that for rippled regimes (as was observed during PIPESTAB storm measurements) the spectral wave friction does not increase as drastically (according to Jonsson and Carlsen (1976) formula) as for monochromatic waves. This can be clearly seen in Fig. 8, where the results of computations for Madsen's et al. (1990) laboratory data (irregular waves, symbol +) approach the field measurements of Myrhaug et al. (1992).

3.3. Nonlinear (Asymmetric) Waves

In the modelling of roughness parameter under asymmetric wave the iterative method described in section 2.3 has been used, as in the case of sinusoidal wave, considered in section 3.1. The numerical solution of Equation (22), proposed by Fredsoe (1984) for sinusoidal wave, has been adapted for the case of nonlinear (asymmetric) wave. The free stream velocity $U(\omega t)$ has thus been expressed using nonlinear approximation. The 2nd and 3rd Stokes cases have been examined.

Figure 11 shows the relative difference of the roughness parameter k_a for linear and 2nd Stokes theories. It is obvious that the greatest reduction of k_a, amounting up to 40%, takes place for the depth-to-wavelength ratio $h/L = 0.10$.

The case of $h/L = 0.10$ has therefore been tested thoroughly to perform the comparisons of the roughness parameter for a number of cases: sinusoidal, nonlinear (2nd and 3rd Stokes theory) and irregular. The computational results are plotted in Fig. 12, as well as the relative differences for all cases with respect to the linear (sinusoidal) one. It can be seen that the most significant k_a reduction is obtained for random (irregular) waves and is almost constant, independent of Shields' parameter, amounting to about 40%.

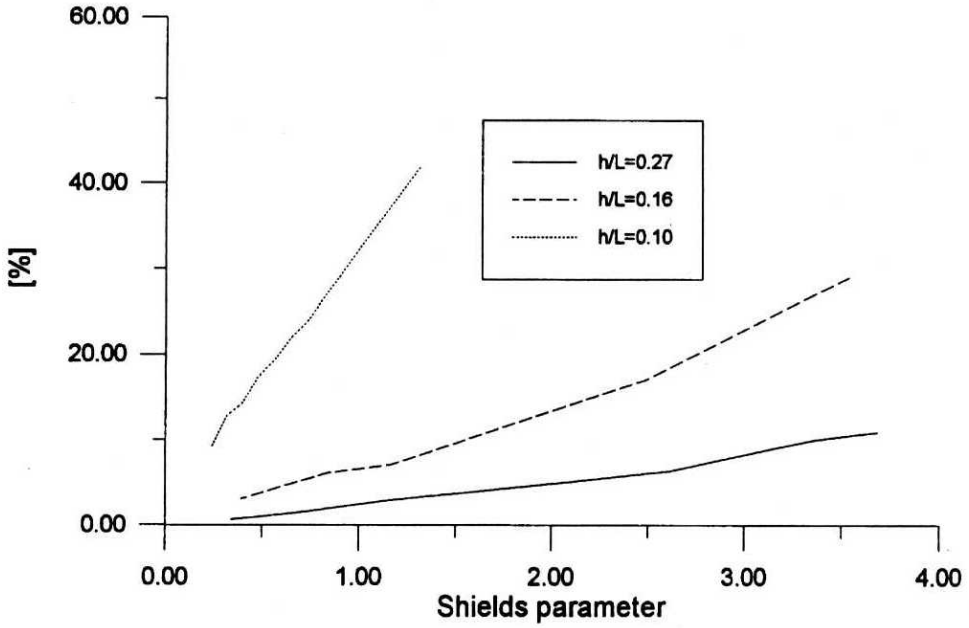

Fig. 11. Relative difference of roughness parameter k_a for linear and 2nd Stokes theories

It should be noted that the computational results for nonlinear and random waves in Figs. 11 and 12 have been plotted as the functions of Shields' parameter corresponding to their sinusoidal counterparts.

3.4. Waves and Currents

The cases of sinusoidal and asymmetric waves with/versus a steady current have been considered. In the modelling of roughness parameter under wave and current the iterative method described in section 2.3 has been used, similar the cases considered in the sections 3.1 and 3.3. The numerical solution of Equation (23), proposed by Fredsoe (1984) for sinusoidal wave and current, has been adapted for the case of nonlinear (asymmetric) wave, similar to as for the case of nonlinear wave without a current. The free stream velocity $U(\omega t)$ has thus been expressed using nonlinear approximation. The considerations on nonlinearity have been limited to the 2nd Stokes wave proparting with/against weak and strong currents. The

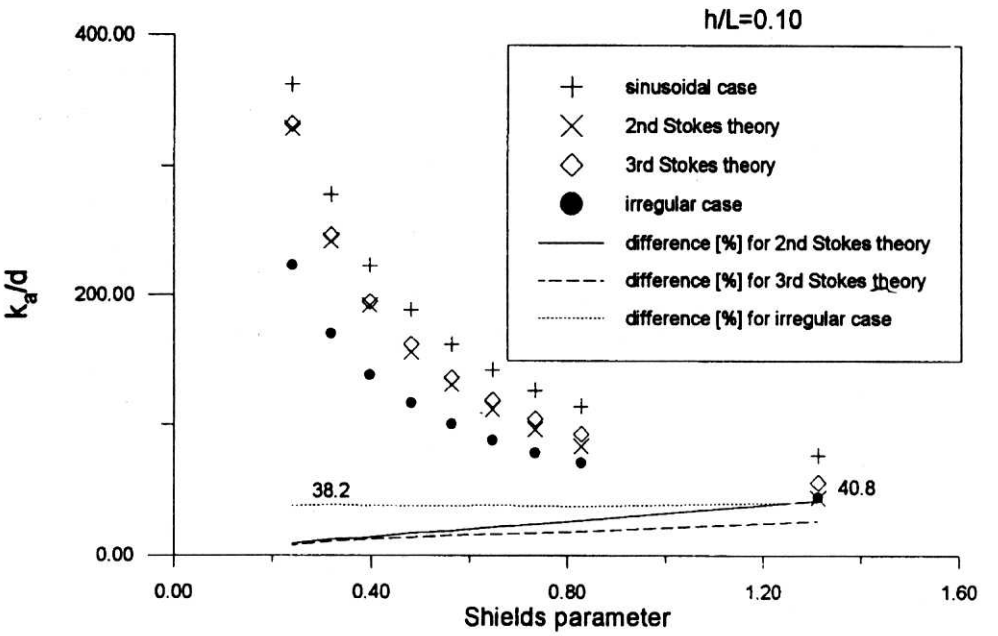

Fig. 12. Roughness parameter k_a and its relative differences for linear, nonlinear and irregular waves

ratio U_{mean}/U_{1m} was kept constant and amounted to 0.2 and 0.5 for weak and strong current, respectively. The quantity U_{mean} is the steady current, known as an input, averaged over water depth in the outer region (outside the bed boundary layer). The mean slip velocity (at the top of the bed boundary layer) is calculated from U_{mean} with the assumption of the logarithmic velocity profile in the outer region, using the model of Kaczmarek and Ostrowski (1992).

It should be noted that the friction velocity u_{f0} in Equation (23), representing the shear stress at the top of the boundary layer – resulting from the steady current, is basically unknown. For its determination the computational method proposed by Kaczmarek and Ostrowski (1992) has been used.

Fig. 13 depicts the relative differences in roughness computed for waves (linear and nonlinear) and currents with respect to pure sinusoidal cases. For the sake of complete comparison the case of irregular wave has also been included in the plot.

The results shown in Fig. 13 imply that the greatest reduction of the roughness parameter k_a (about 40%) is observed when the waves are irregular and – in a certain range of Shields' parameter – when the nonlinear waves are accompanied by a steady current (20–40%). Smaller reduction of k_a (not exceeding 10%) occurs in sinusoidal wave and strong current cases while it is negligibly small for sinusoidal wave and weak current. It should also be pointed out that for nonlinear case the

reduction of k_a is greater for waves propagating with the current than for waves versus the current.

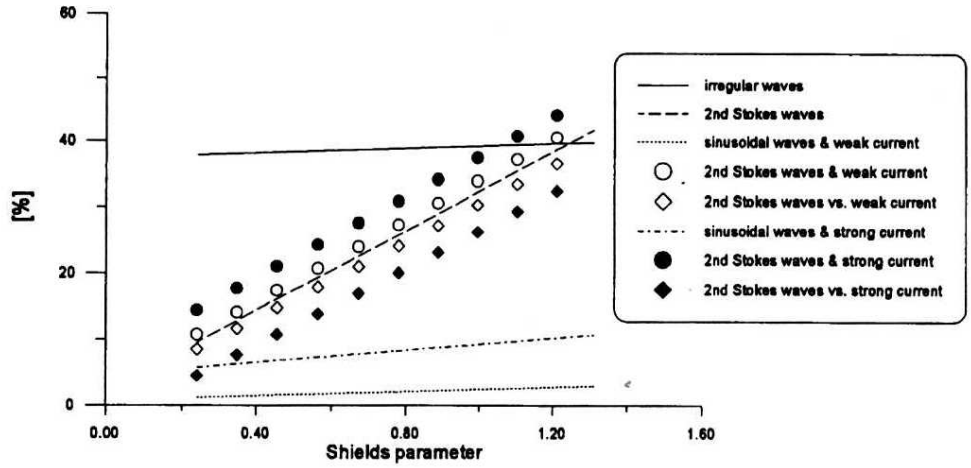

Fig. 13. Relative differences in roughness determination [%] with respect to sinusoidal case: $h/L = 0.10$ (smoothed values)

4. Conclusions

A new theoretical approach based on the grain-grain interaction ideas is proposed for the evaluation of moveable bed roughness under regular and irregular waves, sinusoidal/asymmetric waves with/versus currents.

The present findings for regular waves propagating over plane or rippled bed can be summarized by the following equation:

$$\tau_{\max 1,2} = F_{1,2}[U_{1m}, T, k_a = f(\tau_{\max 1}, s, d)] \tag{34}$$

where subscripts 1 and 2 refer to plane and rippled beds, respectively, U_{1m} is the maximum free stream velocity, T is the wave period, k_a is the moveable bed roughness, $\tau_{\max}$ is the maximum shear stress during the period, s is the specific grain density (2.66) and d is the grain diameter. The function f in Equation (34) is described by the interative procedure presented in section 2.3, the results of which yield the following simplified formula:

$$\log\left[\frac{k_a}{d}\right] = -0.95 \log[\theta_{\max 1}] + 4.55 \tag{35}$$

where the Shields' parameter is calculated using Fredsoe's (1984) model.

To calculate the function F, Fredsoe's (1984) boundary layer model is recommended in the case of a flat bed ($F_1 \rightarrow \tau_{\max 1}$), while the empirical formula of

Kamphuis (1975) or semi-empirical equation of Jonsson and Carlsen (1976) are postulated for the rippled bed equations ($F_2 \rightarrow \tau_{\max 2}$) in order to include the effects of the vortices formed in the lee of the roughness element crest on to turbulent mixing.

The bed friction changes between mono-frequency and random wave conditions. By analogy to the relationship for a monochromatic wave, shown above, one may expect the following relationship between the irregular input specified by the root-mean-square free stream velocity amplitude U_{rms} (equal to $\sqrt{2}$ times the standard deviation, σ_U, of the free stream velocity series) and the irregular output specified by the root-mean-square bed shear stress amplitude τ_{rms} (equal to $\sqrt{2}$ times the standard deviation, σ_τ, of the bed shear stress series):

$$\tau_{rms1,2} = F_{1,2}\left[U_{rms}, T, k_a = f\left(\frac{3\tau_{rms1}}{\sqrt{2}}, s, d\right)\right] \tag{36}$$

where the subscripts 1 and 2 again refer to the plane and rippled bed, respectively.

The value T_r is the period of the monochromatic wave which represents the random wave field. The question of which equivalent wave period to choose to represent the spectral wave conditions is not discussed here. Further information on choosing the representative period can be found in Kaczmarek at al. (1994) and Kaczmarek and Ostrowski (1994), where a $k - \epsilon$ boundary layer model and a combination of Fredsoe's (1984) and Brevik's (1981) solutions, respectively, were used to study the best representative wave. Based on Gdańsk laboratory data Kaczmarek and Ostrowski (1994) found that the representative period equals the peek period.

The function f is expressed using the computational procedure (given in Fig. 10), which incorporates the iterative method described in section 2.3 and may be represented by the approximating formula:

$$\log\left[\frac{k_a}{d}\right] = -1.05\log[\theta_{rms}] + 4.00. \tag{37}$$

The above approximation differs from that given for monochromatic waves due to the largest waves causing a reduction in the roughness parameter.

In an attempt to explain the reduction of spectral wave friction factors the present theoretical approach was run with Madsen et al. (1990) laboratory data. The agreement between theoretical and experimental results appears to be satisfactory.

The various aspects of the nonlinearity in respect to moveable bed roughness have been discussed including the asymmetry of waves (described by second and third Stokes theory) and the interactions between asymmetric waves and/versus currents.

The present results imply that the greatest reduction of the roughness parameter k_a (about 40%), for all shear stress conditions, is observed when the waves

are irregular and – for large waves – when the nonlinear wave motion is accompanied by a steady current (20–40%). Smaller reduction of k_a (not exceeding 10%) occurs in sinusoidal wave and strong current case while it is negligibly small for sinusoidal wave and weak current. It should also be pointed out that for nonlinear case the reduction of k_a is greater for waves propagating with the current than for waves versus the current.

Finally, it can be concluded that the irregularity of waves is the most important factor causing the reduction of moveable bed roughness. Smaller decrease of the roughness parameter can be expected due to wave nonlinearity (asymmetry) while the nonlinearity resulting from wave-current interaction has the smallest influence on bed roughness.

Acknowledgements

The study has been sponsored by KBN under the programme 2 IBW PAN and partially – by British Council, under the British-Polish Joint Collaboration Programme. The author wishes to thank the sponsors for the financial support necessary to complete the study. The author is also grateful to Prof. R. Zeidler for his support during the project, as the supervisor of the 2 IBW PAN programme.

References

Brevik I. (1981), Oscillatory rough turbulent boundary layers, *J. Waterway, Port, Coast. and Oc. Engineering, ASCE,* Vol. 12, No. 5.

Fredsoe J. (1984), The turbulent boundary layer in combined wave and current motion, *J. Hydraulic Eng., ASCE,* Vol. 110, No. HY8.

Horikawa K., Watanabe A., Katori S. (1982), Sediment transport under sheet flow condition, *Proc. 18th Coastal Eng. Conf., ASCE,* Cape Town, South Africa.

Jonsson I. G., Carlsen N. A. (1976), Experimental and theoretical investigations in an oscillatory turbulent boundary layer, *J. Hydr. Res.,* Vol. 14, No. 1.

Kaczmarek L. M., Ostrowski R. (1992), Dynamics of wave-current bottom boundary layer, Part 1: Modelling turbulent boundary layer in nonlinear wave motion, *Archives of Hydro-Engineering,* Vol. XXXIX, No. 1, Gdańsk.

Kaczmarek L. M., Ostrowski R. (1992a), Dynamics of wave-current bottom boundary layer, Part 2: Modelling turbulent boundary layer in nonlinear wave and current motion, *Archives of Hydro-Engineering,* Vol. XXXIX, No. 1, Gdańsk.

Kaczmarek L. M., Ostrowski R. (1992b), Modelling of wave-current boundary layer in the coastal zone, *Proc. 23rd Int. Conf. on Coast. Engng.*

Kaczmarek L. M., O'Connor B. A. (1993a), A new theoretical approach for predictive evaluation of wavy roughness on a moveable-flat bed, *Report CE/14/93,* Department of Civil Engineering, University of Liverpool.

Kaczmarek L. M., O'Connor B. A. (1993b), A new theoretical approach for predictive evaluation of wavy roughness on a moveable rippled bed, *Report CE/15/93,* Department of Civil Engineering, University of Liverpool.

Kaczmarek L. M., Harris J. M., O'Connor B. A. (1994), Modelling moveable bed roughness and friction for spectral waves, *Proc. 24th Int. Conf. on Coast. Engng.*

Kaczmarek L. M., Ostrowski R. (1995), Modelling of bed shear stress under irregular waves, *Archives of Hydro-Engineering and Environmental Mechanics* (submitted for publication), Gdańsk.

Kamphuis J. W. (1975), Friction factor under oscillatory waves, *J. Waterways, Harbours and Coastal Eng. Div., ASCE,* Vol. 101, No. WW2.

Madsen O. S., Poon Y-K., Graber H. C. (1988), Spectral wave attenuation by bottom friction: Theory, *Proceedings of the 21st International Conference on Coastal Engineering,* Malaga, ASCE, Chapter 34.

Madsen O. S., Mathison P. P., Rosengaus M. M. (1990), Moveable friction factors for spectral waves, *Proc. 22nd Int. Conf. on Coast. Engng., ASCE.*

Myrhaug D., Lambrakos K. F., Slaattelid O. H. (1992), Wave boundary layer in flow measurements near the sea bed, *Coastal Engineering,* 18.

Nielsen P. (1992), Coastal bottom boundary layers and sediment transport, *Advanced Series on Ocean Engineering,* Vol. 4.

Ockenden M. C., Soulsby R. L. (1994), Sediment Transport by Currents Plus Irregular Waves, *Report SR 376,* HR Wallingford.

Oebius H. U. (1992), Circulation and Sediment Transport on Sand-Banks in European Shelf Seas, Part: Development of a shear stress Meter, *Report No. 1208/92,* VWS, Berlin, 100 p.

Sayed M., Savage S. B. (1983), Rapid gravity flow of cohesionless granular materials down inclined chutes, *J. Applied Mathematics and Physics (ZAMP),* Vol. 34.

Soulsby R. L., Davies A. G., Wilkinson R. H. (1983), The detailed Processes of Sediment Transport by Tidal Currents and by Surface Waves, *Institute of Oceanographic Sciences Report No. 152,* 80 p.